We are IntechOpen, the world's leading publisher of Open Access books
Built by scientists, for scientists

5,600
Open access books available

137,000
International authors and editors

170M
Downloads

Our authors are among the

154
Countries delivered to

TOP 1%
most cited scientists

12.2%
Contributors from top 500 universities

CLARIVATE ANALYTICS
BOOK CITATION INDEX
INDEXED

WEB OF SCIENCE™

Selection of our books indexed in the Book Citation Index
in Web of Science™ Core Collection (BKCI)

Interested in publishing with us?
Contact book.department@intechopen.com

Nanocomposite and Nanofluids: Towards a Sustainable Carbon Capture, Utilization, and Storage

Ronald Nguele, Katia Nchimi Nono and Kyuro Sasaki

Abstract

Large volumes of unconventional fossil resource are untapped because of the capillary forces, which kept the oil stranded underground. Furthermore, with the increasing demand for sustainable energy and the rising attention geared towards environment protection, there is a vital need to develop materials that bridge the gap between the fossil and renewable resources effectively. An intensive attention has been given to nanomaterials, which from their native features could increase either the energy storage or improve the recovery of fossil energy. The present chapter, therefore, presents the recent advancements of nanotechnology towards the production of unconventional resources and renewable energy. The chapter focuses primarily on nanomaterials applications for both fossils and renewable energies. The chapter is not intended to be an exhaustive representation of nanomaterials, rather it aims at broadening the knowledge on functional nanomaterials for possible engineering applications.

Keywords: nanoparticle, nanocomposite, oil recovery, CO_2 sequestration, solar energy

1. Introduction

Metal Oxides (MO) are a class of compounds that are as abundant in the nature than in the library of synthetic inorganic compounds. While the use of MO as bulk materials is widely applied, developing new class of materials based on MO, understanding their chemistry, tuning their characteristics, and developing novel potential engineering are still under investigation. MO nanoparticles (MO-NP) are MO with a diameter ranging between 10 and 100 nm with a high surface-to-volume ratio, which explains their advantageous features compared to similar materials of micro- or macro-size [1].

MO-NPs can contain either a single metallic specie (nanoparticle, NP) or two or more different metallic species (nanocomposite, NCP). When the metal species are separated and independent at the molecular level, the nanocomposites could refer to a simple mixture of oxides with several component phases. In some systems, nanocomposites consist in stoichiometric (or non-stoichiometric) replacement of a metal ion by another one in the first oxide crystallographic structure. Such substitution systems are referred as mixed MOs e.g. spinels [2] or perovskites [3, 4].

MO-NPs also include core-shell architectures where each particle has an inner core made of one type of MO, and the outer shell consisting in another MO. Just as single nanoparticles, composite nanoparticles exhibit size confinement properties (optical and electronic). Their composition and the atomic order of aggregates are pivotal factors for their specific features, which are tailored during their synthesis. MO-NPs have a high surface-to-volume ratio, which increases the reactivity. Dispersed in base fluid (BF), MO-NP enhances the native properties of the solution compared to the case in which no MO-NPs were added.

This chapter does not intend to list, in an exhaustive manner, the features of nanofluid. Rather, the authors aim to discuss, from both the chemistry and the engineering point of view, the key features of MO-NFs transferable to the carbon capture utilization and storage (CCUS). The chapter will cover the different synthesis methods of the NP and NCP, the formulation of NF as well as the application in respect of CCUS.

2. Synthesis of MO-NPS and MO-NCPs

MO-NPs can be obtained through two opposite approaches including top-down and bottom-up. The former technique consists in successive mechanical operations of divisions and fragmentations, or in the irradiation of the bulk phase with a powerful energy source including UV, X-Rays, electron beam [5]. Using the bottom-up approach, MO-NPs are formed within the reaction medium, subsequently to the clustering of single atoms. The growth in size is time-dependent, and may be facilitated by additional treatment such as calcination [6].

2.1 Physical methods

2.1.1 Spray pyrolysis

Spray pyrolysis is generally used for the preparation of thin-films or pulverulent materials. It consists in the spraying of a solution or a suspension containing the metallic precursors in an oven, followed by a high temperature treatment. This method allows the formation of spherical oxides as the shape of the oxides are strongly dependent of the drops generated at the entrance of the furnace. Given the rapid rate of nucleation at high temperature, there is a one-droplet, one-particle mechanism.

In addition to the shrinkage occurring following the formation of oxides, micrometers precursors can allow the formation of particles in the nanometer size range [7]. NCPs can also be obtained through this method by mixing several metal ions in the precursor solution. The formulation of the composites is controlled by adjusting the stoichiometric proportions of each metallic species in the solution [8, 9].

2.1.2 Chemical vapor deposition (CVD)

This technique is used mostly for the preparation of 2D metallic or inorganic materials of nanometric thickness. Usually, volatiles precursors are delivered on a heated surface on which a thin layer of materials is deposited upon a chemical reaction in vapor phase. Additional physical processes such as evaporation or sputtering are usually required to complete the synthesis.

During the preparation of MOs by CVD, oxidation and hydrolysis are the primary chemical reactions taking place in the presence of oxidizing agents (oxygen or ozone) and the precursors are usually metal alkoxides [10].

2.1.3 Sonochemistry

Sonochemistry is a branch of chemistry supported by the formation, growth, and collapse of bubbles in a liquid upon irradiation with high intensity ultrasound waves. The bubbles can reach a temperature and pressure as high as 5000°C and 500 mPa respectively [11]. These conditions increase the chemical reactivity of the species in the reactor. When the water is the solvent, radical •OH, H_2O_2 and O_3 are generated, leading thereby to oxidant medium suitable for the preparation of MO.

Treatment of solutions of copper (Cu), zinc (Zn) and cobalt (Co) acetates under a high-intensity ultrasonic horn has been used to produce nanosized CuO, ZnO, and CoO_3 respectively [12]. This method has also been used for the preparation of nanocomposite when the suitable precursors are mixed [13].

2.2 Chemical methods

2.2.1 Hydrothermal synthesis

Hydrothermal or solvothermal synthesis (if water is the solvent) is a synthesis method in which the precursors (dissolved or dispersed in water) are placed in an autoclave where the reaction takes place at high temperature and pressure [14]. Hydrothermal allows the synthesis of MO-NPs from a wide variety in shape, size, structure, and composition, provided that key-factors such as temperature, pressure, pH, concentration of reactants are well-controlled [15–20].

2.2.2 Sol-gel synthesis

It involves the hydrolysis and condensation of metal alkoxides, acetates, nitrates, sulfates, and chlorides. Their hydrolysis in solution results from the dispersion of metal hydroxides, which further undergo condensation leading to the formation of 3-dimensional network namely a gel. The gel is either dried by removing the solvent or treated by chemical reaction to give the condensed MO materials [21]. The solvent used is generally water (aqueous sol-gel). In most non-aqueous synthesis, additives such as surfactant can be required to control the morphology of the particles and most importantly to prevent/reduce their aggregation [22, 23].

2.2.3 Co-precipitation

The co-precipitation method entails the co-precipitation of cations in an aqueous media by the addition of an alkaline solution. A short burst of nucleation occurs when the concentration of the species reaches its critical super-saturation, and then, there is a slow growth of the nuclei by diffusion of the solutes to the surface of the crystal. MO-NPs are dried further or sometimes calcined at temperatures above 500°C, in which case there is an alteration of the structure of material [24].

The co-precipitation method can be relevant for the synthesis of both MO-NP and MO-NCP [25]. The size and morphology of the nanoparticles produced by this method can be controlled by varying the molar ratio of the two precursor ions, the base used, mixing rate, the pH, and the temperature [26]. Unfortunately, it produces wastewaters with very basic pH needs to be treated before been discarded.

2.3 Alternative synthesis methods

Most of the methods of synthesis of nanomaterials allow a great flexibility in the choice of the precursors and the morphology of the material through the control of key parameters such as temperature, concentration, or pH. However, they also required the use of toxic chemical reactants or additives. In this regard, alternative synthesis routes have been exploited, with mitigated results, including biosynthesis, plasma assisted. Extraction from ores as for it fits in the strategy of valuation of naturally occurring ores.

2.3.1 Biosynthesis of MOs NPs

This synthetic approach includes the use of vegetal substances (plant extracts or agricultural wastes) but can also involve living organisms such as bacteria and fungi. Natural extracts used for the preparation of the MO materials are available and renewable, in addition to contain organic groups that can react with the metal ions is solution in the absence of further additives [27, 28].

2.3.2 Plasma assisted synthesis

The plasma state is obtained from the ionization of noble gases, which increases the reactivity of the medium rich in electrons and chemical species upon reaching a very high temperature, up to 10000K [29]. Non-thermal plasma is an advantageous alternative that can be operated at atmospheric pressure [30]. Among the different types of systems used for plasma production, gliding arc discharge is reported to attractive for MO-NPs synthesis.

Under humid air as feeding gas, glidarc discharge produces acidic and very oxidizing environment in which many transitions metal ions precipitate as hydroxides or oxides [31–33]. However, one of the major disadvantages associated to this technique is the poor control on the size range and morphology of the particles.

2.3.3 Extraction from ores

Mineral ores are naturally occurring rock, from which the metal content can be extracted via hydrometallurgy [34]. During MO extraction, the ore is successively crushed, roasted, leached, and precipitated. The leaching step consists in the solubilization of the metal species under its ionic forms by the action of a strong acid or a strong base. Usually, impurities remain insoluble and are removed from the mixture.

The metal ions remaining in solution are then concentrated by solvent (water) evaporation before further treatment for the precipitation. When the mineral contains one major species, single MO particles are produced, but for more complex ore, composite materials can be obtained [35, 36].

3. Preparation and stability of metal oxide nanofluid

3.1 Preparation

Preparation of NFs is the most challenging step, as far as the experimental studies with NFs are concerned. This is so because nanofluids need special requirements

including stable suspension, low agglomeration of particles, and no chemical change of the fluid.

3.1.1 Preparation using direct method or one-step approach

One-step technique (or direct approach) consists in formulating the nanofluid right after their synthesis. The literature reports two major approaches including direct evaporation and the laser ablation method. In either approach, the nanofluid is obtained after a transition from the gas to solid phase [37, 38].

3.1.2 Preparation using two-step method approach

Two step approach is designed in a manner that the surface of MO-NPs is sufficiently wet so to mitigate the particle impingement [39]. This is done by either using mechanical mixing [40] or sonication or the combination of both [41, 42] as shown in **Figure 1**.

During the mechanical mixing, the large flocs are broken down and the individual particles are kept separated from each other. During the sonication stage, the ultrasound waves, by stretching the molecular spacing of fluid, creates cavities within, which cause subsequently the chemical bonds to break [44]. However, due to the intrinsic properties of MO-NPs, a poor dispersion is often yielded which is mitigated by either extending the mixing time, adding few drops of acidifying agents [45] or even bubbling gas during the preparation [43].

3.2 Stability of MO-NFs

3.2.1 Monitoring the stability of NFs

3.2.1.1 Sedimentation and centrifugation method

Sedimentation method is the simplest and most straightforward method to investigate the stability of a nanofluid. A fixed volume of nanofluid is transferred into a graduated test tube and observed over the time. **Figure 2** shows the sedimentation of alumina-based NFs upon increasing the load in NPs.

The monitoring of the volume of deposited NPs showed that a load in alumina-NP of 0.05 wt.% was sufficient to give a stable nanofluid. The literature reports similar results, in which no or little visual sedimentation of particles can be observed from the naked eye [46].
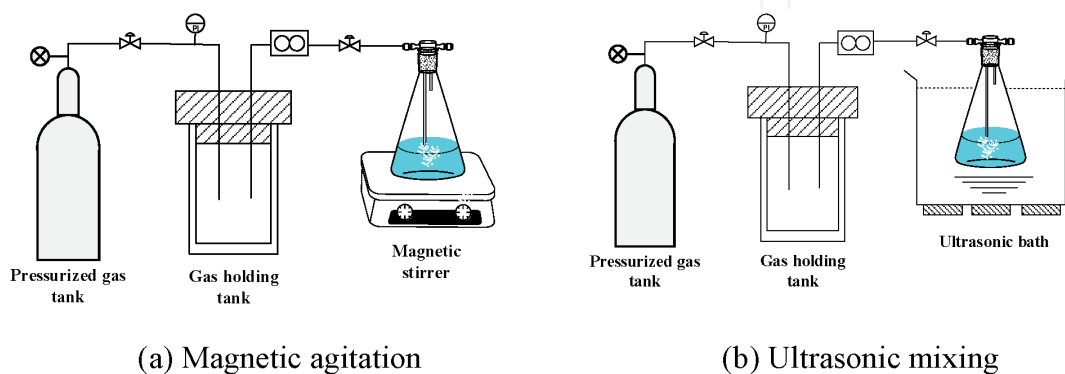

(a) Magnetic agitation   (b) Ultrasonic mixing

Figure 1.
Preparation of polymer-based NFs; Adapted with permission from [43]. Copyright (2019) American Chemical Society.
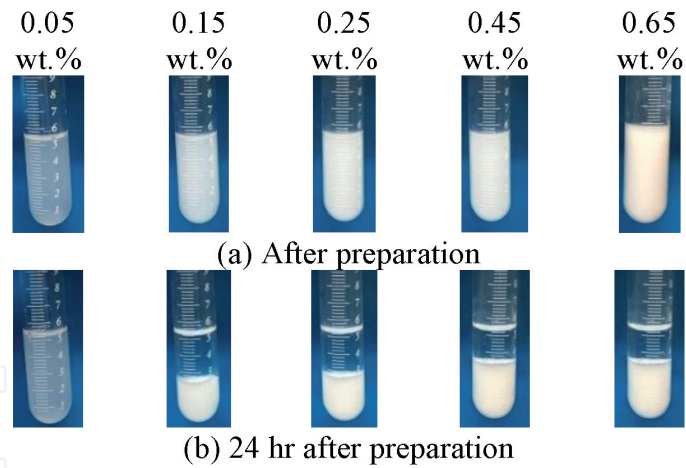
Figure 2.
Sample pictures of water-based NFs prepared using alumia oxide NPs and ethylene glycol as BF.
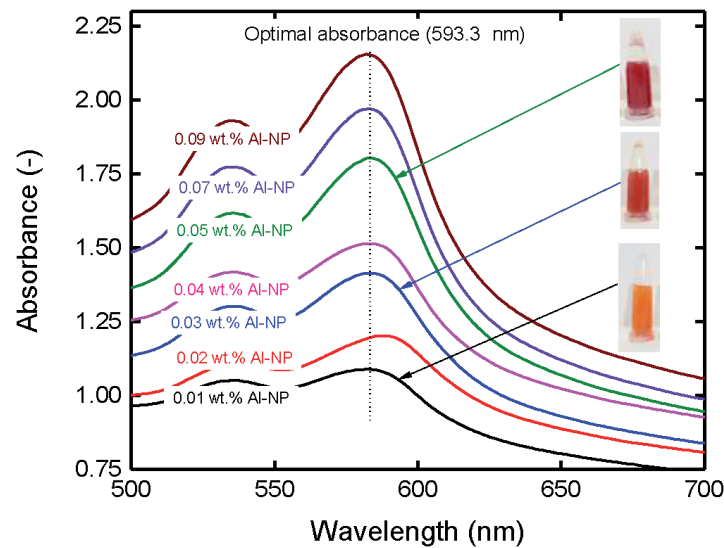

Figure 3.
Monitoring alumina-based NFs stability using UV-Vis spectroscopy and 1-(-2pyridylazo)-2-naphthol, PAN. Adapted with permission from [47]. Copyright (2020) American Chemical Society.

3.2.1.2 Spectrophotometric analyses

This approach relies on the intensity of absorption when the light passes through a target sample. As shown in **Figure 3**, Ngo et al. monitored the stability of alumina-based nanofluid by combining colorimetry and spectrophotometry [47].

3.2.1.3 Other monitoring methods

Another straightforward approach for monitoring the nanofluid stability is to measure the particle size at different time intervals. This could be achieved by either using scanning/transmitting electron micro- scope (SEM/TEM) or zeta potential [48]. SEM/TEM allows to directly visualize the distribution of particle size and the evolution of particle coagulation. Easy and fast, SEM/TEM does not require separation of NP from the solvent [49].

As far as colloidal suspensions are concerned, Zeta potential defines the electro kinetic potential in a nanofluid. It indicates the interaction energy between

particles. High absolute value of zeta potential means stronger repulsive force between NPs, and hence indicates better stability of nanofluid.

3.2.2 Enhancing the stability of nanofluid

The stability of NF is fully acquired when there is a minimization of the surface area of the NPs dispersed in the solution. To prevent the particle agglomeration, an energy barrier must be created to prevent them from passing the unstable to stable energy state. This could be performed by (a) by addition of acidic or alkaline materials, (b) altering the preparation step, and (c) choosing a proper BF [50–52].

Figure 4 shows the influence of the preparation step of nanofluid stability.

The results showed that the acidity of the solution decreases regardless the preparation method. However, combing both the sonication and the magnetic stirring could prolong the stability of the nanofluid. Furthermore, Nguele et al. [43] and later Ngo et al. [47] reported that bubbling gas during the preparation could further enhance the stability regardless the type of base fluid (**Figure 5**).

The average decrease in acidity of about 20 % from the initial value (pH =5.4) was observed throughout the preparation stage when CO_2 gas, which contrasts with an increase in pH twice higher when O_2 was bubbled. Regardless the reason pertaining to the increase in pH (i.e., carbonation for CO_2 bubbling and radical formation for O_2 bubbling), the surface modification of NP and thus the stability is enhanced.

The addition of dispersants is an alternative for enhancing the stability of NFs [48, 50, 53]. These dispersants attach to the surface of the NP due to the mutual affinity. In addition, the tail of the attached dispersant works as a steric barrier, which prevents the particles from agglomerating. Such effect, known as steric hindrance, inhibits the coagulation of NPs in the suspensions (**Figure 6**).
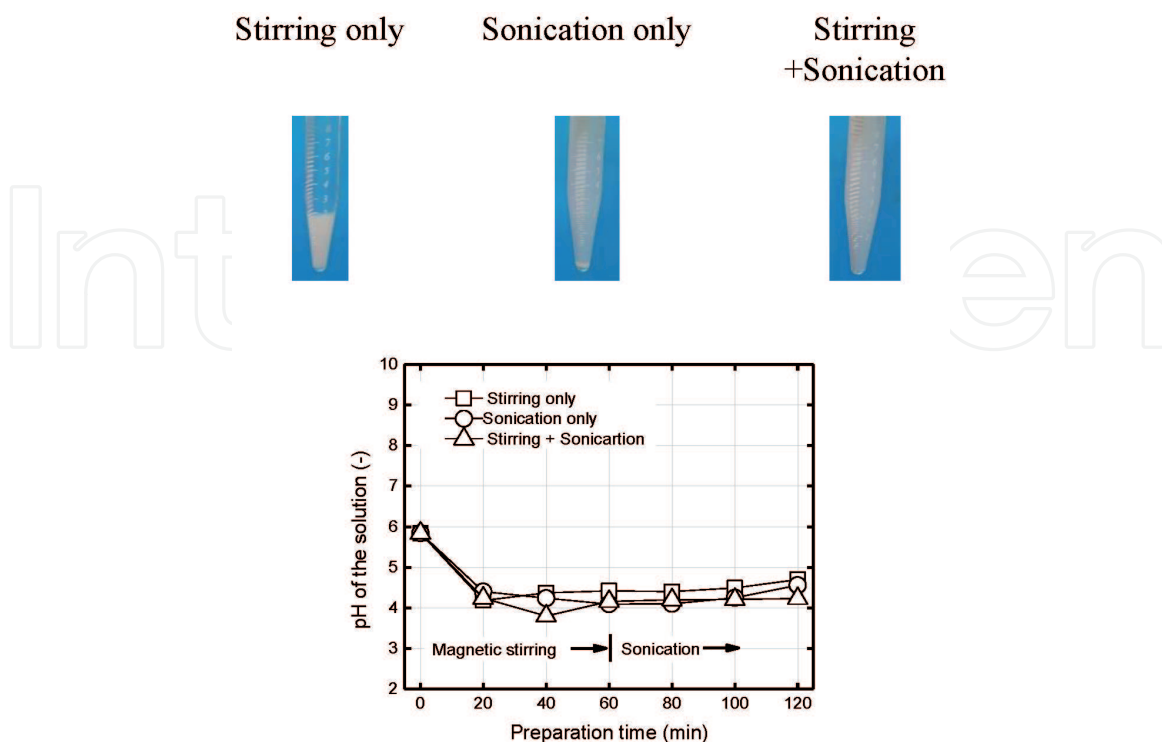

Figure 4.
Influence of preparation step on the stability of nanofluid; the nanofluid consists in Si-NP dispersed in an aqueous polymeric solution, Reprint with permission from [43] Copyright (2019) American Chemical Society.
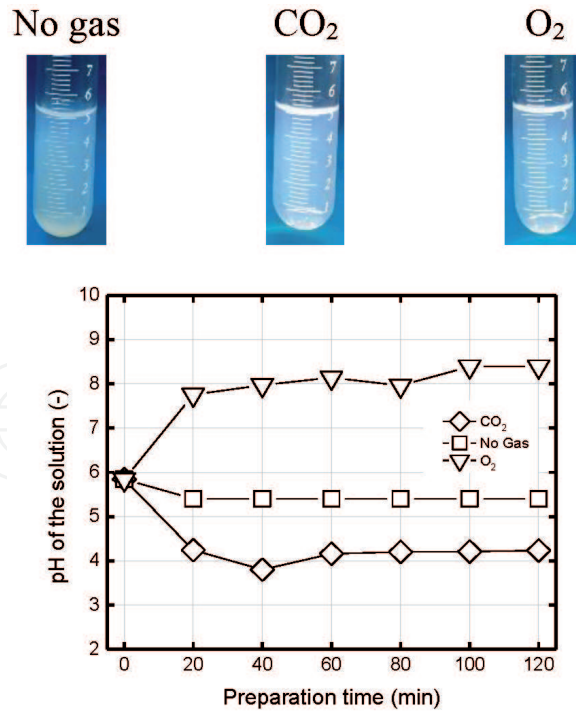
Figure 5.
Influence of gas bubbling on the stability of nanofluid; the nanofluid consists in Si-NP dispersed in a deionized water.

(**a**) PVOH-1   (**b**) PVOH-2   (**c**) PVOH-3   (**d**) PVOH-4
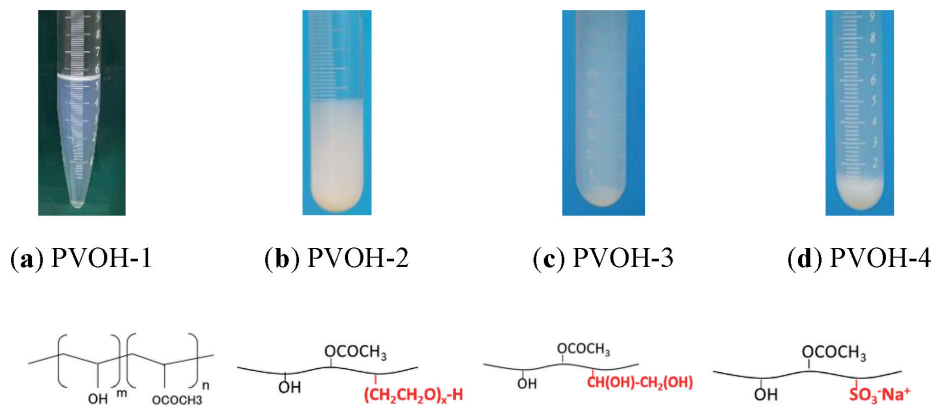

Figure 6.
Influence of BF on the stability of nanofluid at 25°C; the nanofluid consists in Si-NP dispersed in a polymer (PVOH) solution prepared following two-step approach using CO_2 bubbling.

4. Application of MO-NFs to fossil, gas storage and renewable energy

4.1 Fossil energy and enhanced oil recovery (EOR)

4.1.1 Tertiary oil recovery

Improved oil recovery (IOR) or enhanced oil recovery (EOR) are two terms used loosely to describe the improvement of oil recovery after both the primary and the secondary stages of oil production become economically unattractive or technically not feasible. In principle, IOR is the general term to designate any implemented means after secondary process that increases considerably the amount of oil recovered. On the hand, EOR defines a specific technique (or a combination of techniques) implemented to decrease the residual oil.

EOR methods are grouped into thermal and non-thermal methods. Thermal methods are the most advanced techniques among EOR methods and are best suited for heavy oils and tar sand formations. In these methods, the heat is supplied to the reservoir in form of steam or fire, which favors the vaporization of stranded oil. The major drawbacks associated to thermal-EOR pertain to the geometry and the petrophysical properties of the candidate formation [54].

Non-thermal methods encompass techniques that reduce the interfacial tension (IFT) between the stranded oil and resident fluids and the viscosity of the oil. Among the most prominent methods, gas-EOR stands out because of it offers the possibility to sequester greenhouse gases. During a gas-EOR, the injected gas dissolves into the oil after a first (or multiple) contact leading to a foamy oil, whose viscosity is lower than that of the original oil [55]. Often, gas-EOR is challenged, in part by, the deposition of heavy fractions [56–58].

If the slug is a surfactant [59], a polymer [60], or even a micellar solution [61], the oil is produced by reduction of IFT or wettability. Major problems associated to surfactant-EOR are the loss of chemical, phase partitioning and trapping, and the slug by passing. Unlike chemical-EOR, microemulsion-EOR relies on the reduction of the mobility ratio. Microemulsions, kinetically more stable than emulsions, are potentially viable because of the ultra-low IFT and their high interfacial area [62–64].

Microbial-EOR uses the potential of microbes to yield either bio-surfactant, slimes (polymers), biomass and/or gases such as CH_4, CO_2, N_2 and H_2 as well as solvents and certain organic acids [65, 66]. Oil recovery mechanisms in microbial-EOR are like those of the classic chemical methods. This includes IFT reduction, emulsification, wettability alteration, improved mobility ratio, selective plugging, viscosity reduction, oil swelling and increased reservoir pressure due to the formation of gases [67, 68].

Nano-EOR has been reported to be the next generation of EOR, which is evidenced by the wealth in literature covering the topic [69–75]. Therefrom, it appears that the mechanisms of oil production using MO-NPs are (1) wettability and the IFT alteration, (2) advanced drag reduction, and (3) the decrease of the mobility ratio.

4.1.2 EOR mechanisms in respect of MO-NPs

4.1.2.1 Wettability and IFT alteration

Wettability is the preferential tendency of one fluid to wet (or to spread) onto a surface [76]. To produce more oil, the wettability of the oil-water-rock system should be shifted from oil-wet to a water-wet or strongly water wet condition. MO-NPs can adsorb onto the rock surface and form a nanotexture, which contributes to wettability alteration [77]. However, these mechanisms are affected by the formation salinity (**Figure 7**).

At a low salt concentration, the activity coefficient of the salt increases in a manner that the salt molecules sit within the oil phase. With the presence of salt at the interface, the excess surface concentration turns positive from which results a low contact angle (**Figure 7a**) and higher IFT (**Figure 7b**). An oil production scenario in which the salt concentration is large, the salting-out effect seems to prevail [47].

MO-NPs are depleted at the interface and transferred back to oil phase. This breaks the oil-water interface adsorption, hence a high contact angle. The same behavior could be extended when two immiscible liquids (oil and water) meet each
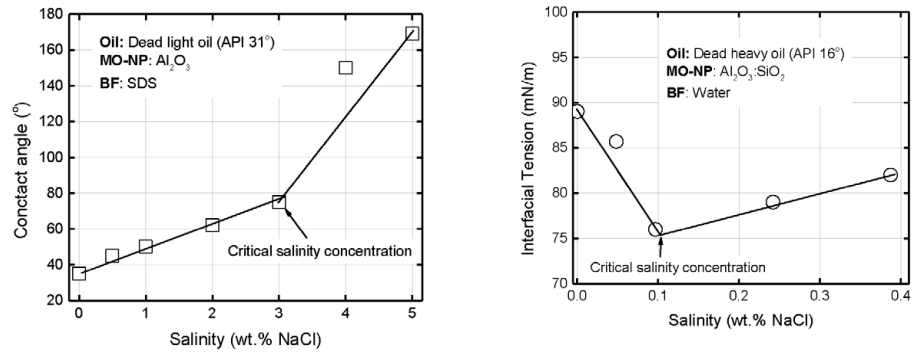
(a) Wettability alteration modified from adapted with permission from [47]. Copyright (2020) American Chemical Society
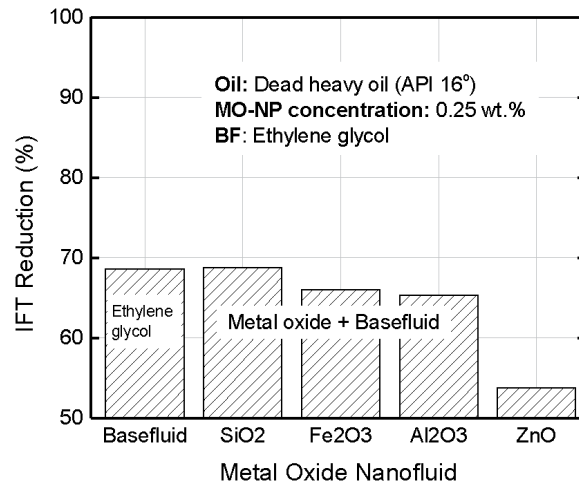
(b) IFT alteration; this study

Figure 7.
Influence formation salinity on wettability and IFT alteration. (a) Wettability alteration modified from adapted with permission from [47]. Copyright (2020) American Chemical Society. (b) IFT alteration; this study.

Figure 8.
Influence of type of MO-NPs on IFT alteration.

other. The molecules at the surface of both of those liquids become unbalanced forces of attraction, which cause the IFT to rise.

Adding MO-NPs could not only reduce the IFT but also the contact angle. For example, it was found adding only 0.25 wt.% of MO-NP to a polymeric BF, the contact angle as well as the IFT between the nanofluid and heavy oil (API 16°) decreases about 50% from its initial value (**Figure 8**).

4.1.2.2 Improve mobility ratio of injected fluids

The mobility ratio of water to oil is one of the most critical factors to influence water flood efficiency. When mobility is greater than one, it is considered unfavorable as the displacing fluid is more mobile than oil in the porous medium; the slug tends to bypass oil and early breakthrough is experienced at the producers (channeling). At a mobility ratio of less than one, water is less mobile than oil leading to better displacement and recovery of oil.

The mobility ratio can be decreased either by reduction of the viscosity of the resident oil or by increasing that of the nanofluid. As shown in **Figure 9**, increasing the load in MO-NP (SiO$_2$-NP in this experiment) prompted an increase in oil recovery in a waterflooded sandstone.
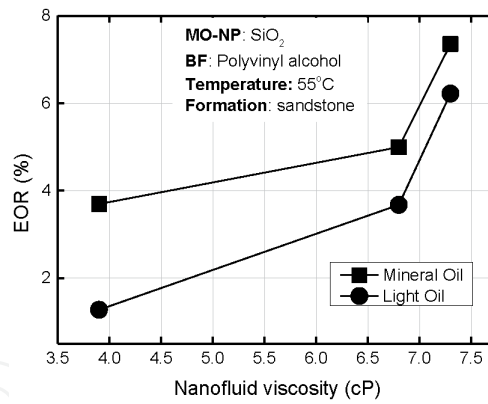
Figure 9.
Relationship between MO-NP viscosity and oil recovery factor.

The experiments were conducted using light mineral (specific density 0.838, viscosity of 26 cP at 25°C) and light crude oil (specific density 0.860 viscosity of 9.54 cP at 25°C). It was found a higher production when light mineral oil was used. This is because of the difference in native composition including a low acid number, a high concentration of asphaltene.

4.1.2.3 Pore channels plugging

Pore channels plugging can be caused by two mechanisms: mechanical entrapment and log-jamming. These mechanisms were evaluated in this study by the injection of Si-NP dispersed in aqueous polymeric solution. Two types of formations were considered including a homogeneous formation with a uniform porosity and a heterogeneous formation with contrasted porosity. The results are shown in **Figure 10**.

The production in homogeneous formation decreases monotonically with the load in Si-NP, while a reverse trend was observed for a heterogeneous model. In a homogeneous formation, the increase in MO-NP load causes the plugging of pore throats, whose size are smaller than the average size in MO-NP dispersed (log jamming). As the nanofluid travels within the formation, the narrowing of flow area and the differential pressure led to a velocity increase of the nanofluid.
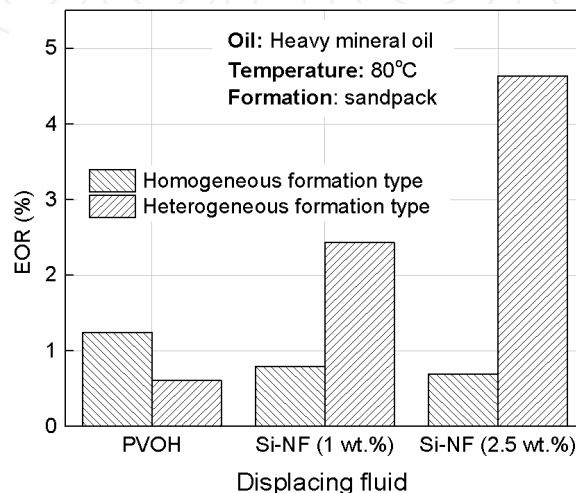

Figure 10.
Oil recovery using Si-NPs in contrasted sandstone formations.

The smaller molecules will flow faster than causing accumulation of MO-NP at the entrance of the pore throats. For larger load, there is a possibility of having a plugging at the entrance of the throat due to the size of the nanofluid (mechanical entrapment). For formations with contrasted porosity, the log-jamming or mechanical entrapment could be beneficial.

As the pore is plugged, there is a pressure build in the adjacent pore throat, forcing out the oil trapped in the pore throat or the water to move to a layer with lower porosity. This can be considered as temporary log-jamming. This phenomenon is mainly governed by the concentration and size of NPs, flow rate and the diameters of pore throats (**Figure 11**).

4.1.2.4 Preventing asphaltene precipitation

Asphaltene precipitation can cause severe problems due to the deposition inside the reservoir, at the wellhead, and/or inside the pipelines. However, it is believed MO-NPs have the potential to inhibit the adsorption and thus delay the deposition [78, 79]. The particles, in contact with the asphaltenes molecules can minimize the interactions asphaltene-asphaltene and/or asphaltene-rock leading therefore to a mitigation (**Figure 12**).

In this regard, MO-NPs are suitable candidates because their inherent properties. In this study, asphaltenes were extracted from dead heavy crude oil (API 16°) as per the procedure discussed by Goual [80]. An asphaltenic solution of 1wt.% was prepared by diluting extracted asphaltenes with toluene. Two set of experiments were conducted at room temperature including porosity impairment (**Figure 13a**) and adsorption on sandstone (**Figure 13b**).
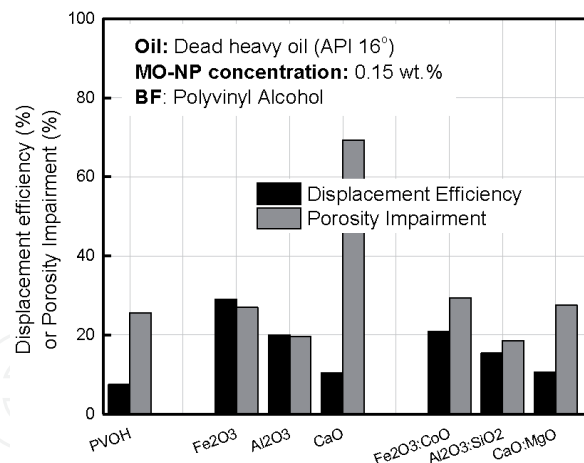

Figure 11.
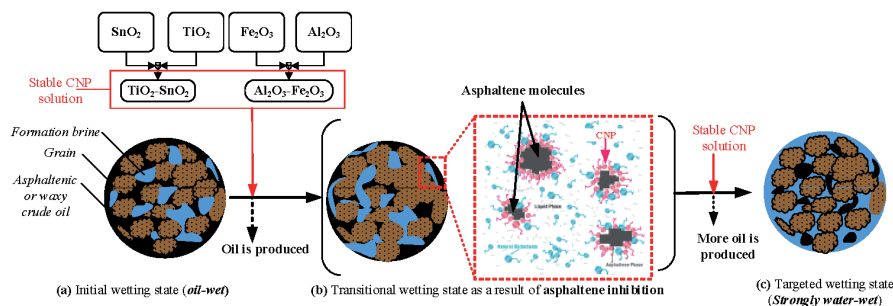*Relationship between the displacement efficiency, porosity impairment and type of MO-NPs.*

Figure 12.
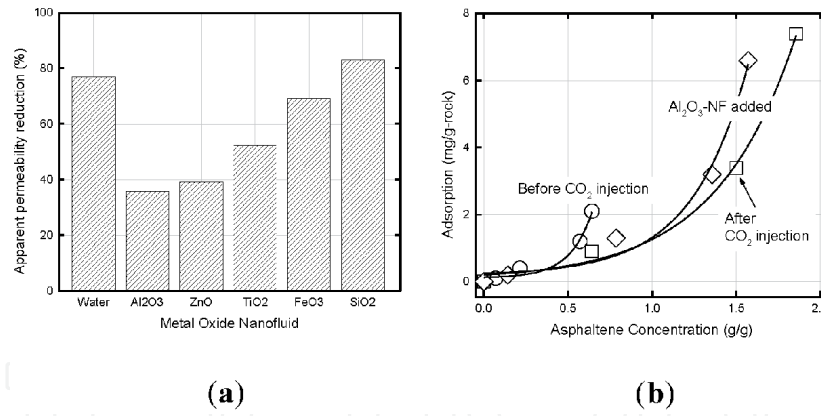*Conceptual approach of asphaltene inhibition during CO_2 injection.*

Figure 13.
Asphaltene mitigation by addition of different types of MO-NPs dispersed into water. (a) Porosity impairment after CO_2 injection. (b) Static adsorption after CO_2 injection.

It could be seen that the porosity of the waterflooded sandstone decreases upon injection CO_2 (**Figure 13a**). Adding MO-NPs to the same water, the impairment could be improved with lowest obtained for Al-NP. This is so because of the higher adsorption capacity of MO-NPs, which interacts more strongly with the asphaltenes. The influence of MO-NP is noticeable as evidenced by the decrease in adsorption (**Figure 13b**).

4.2 Application of MO-NFs to CO_2 Sequestration

As of 2018, 70% of the global warming was subsequent to the release of greenhouse gases (GHG) to the atmosphere, with fossil resources contributing to up to 37.1 billion metric tons. The total concentration in carbon dioxide, CO_2, in the atmosphere was reported to hit its highest level ever (407 ppm) million. Great efforts should be invested to reduce CO_2 concentration to an acceptable value. Carbon dioxide capture, utilization and storage (CCUS) technology of which Carbon capture and storage (CCS) technologies have a potential to reduce CO_2 emissions to the atmosphere due to the huge global capacity for underground storage [81]. With 21 large-scale CCS projects operating worldwide, the volume of storable CO_2 is estimated to be up to 37 Mtpa.

Yet more CCS projects are needed to reach the Paris 2 °C target, which is partly due to the leakage of the stored CO_2 through the faults of the formation within which the gas is trapped [82, 83]. A typical CCS project encompasses the capture, the compression and transport, and the injection in the designed formation. The success of a gas storage depends primarily on the trapping mechanisms occurring during CO_2 containment.

A trapping mechanism refers a process (either physical or chemical), which improves the sequestration of CO_2. Among the different known trapping mechanisms, three processes stand out including residual, solubility and mineral trapping [84]. During the residual trapping, CO_2, injected at its supercritical state, displaces the fluids as it moves through the porous rock. As CO_2 moves upward due to the buoyancy difference, some of the CO_2 will be left behind as disconnected droplets within the pore throats, which are immobile.

This mechanism, however, is challenged by the faults present the geological formation (cap rock). The fault could crack due to the over-pressurization of the aquifer leading to a leak in CO_2 Solubility trapping involves the dissolution of supercritical CO_2 in the salty water (brine), which leads to a fluid denser than the native fluids. From the difference in buoyancy, the resulting fluids force CO_2 to sink at the bottom of formation over time. The problem, in here, is that not only the solubility of CO_2 in brine is low, but it reaches quickly its saturation causing thereby an over pressurization of the aquifer.

Mineral trapping, which is the slowest of the processes, is the final phase. It results from the geochemical reactions of carbonic acid (H_2CO_3) and the native minerals of the formation. This trapping mechanism is dependent on the rock minerals, the pressure of the gas, temperature and porosity of the host formation [85]. However, if mineral trapping is hastened, it may weaken the cap rock and the overlying formation causing a serious leak in CO_2. From above, it appears that the extent to which the CO_2 reacts with the formation water (dominated by its solubility) will vary according to factors such as pressure, temperature, the solubility of CO_2, the fluid and fluid/rock chemistry. The selection of a proper MO-NF could enhance the trapping mechanisms, and ultimately ensure an efficient CO_2 sequestration.

This is potentially achieved by injecting a nanofluid that buffers the acidity within the host formation (**Figure 14b**), but more importantly will yield a gel-like material (**Figure 14a**), denser than the resident fluid in the host formation.

In this study, it was found that formulating a nanofluid from Si-NP and polyvinyl alcohol under CO_2 bubbling would lead to the formation of silicated gels. Increasing the load in Si-NP yields a rigid gel (**Figure 15**).

The results suggest that condensation of SiO_2-NF depends rather on the load in Si-NP than the concentration in PVOH. However, further investigations are required to understand the extent to which the host formation-fluid chemistry alters the solubility of CO_2, and the host formation parameters (fluid chemistry, temperature, and pressure) alter the gel formation.

4.3 Renewable energy production

4.3.1 Overview of photo thermal energy production

Up to date, the primary energy supplied for human needs comes from fossil and nuclear resources. These can be harmful to environment because they cause global warning, ozone layer depletion, biosphere and geosphere destruction, and ecological devastation [86]. These drawbacks have geared the attention towards cleaner energy. Solar energy is one of the most promising amongst them not only because its exploitation can fulfill the entire world demand in energy, but more importantly it is one of the cleanest source or energy [87].
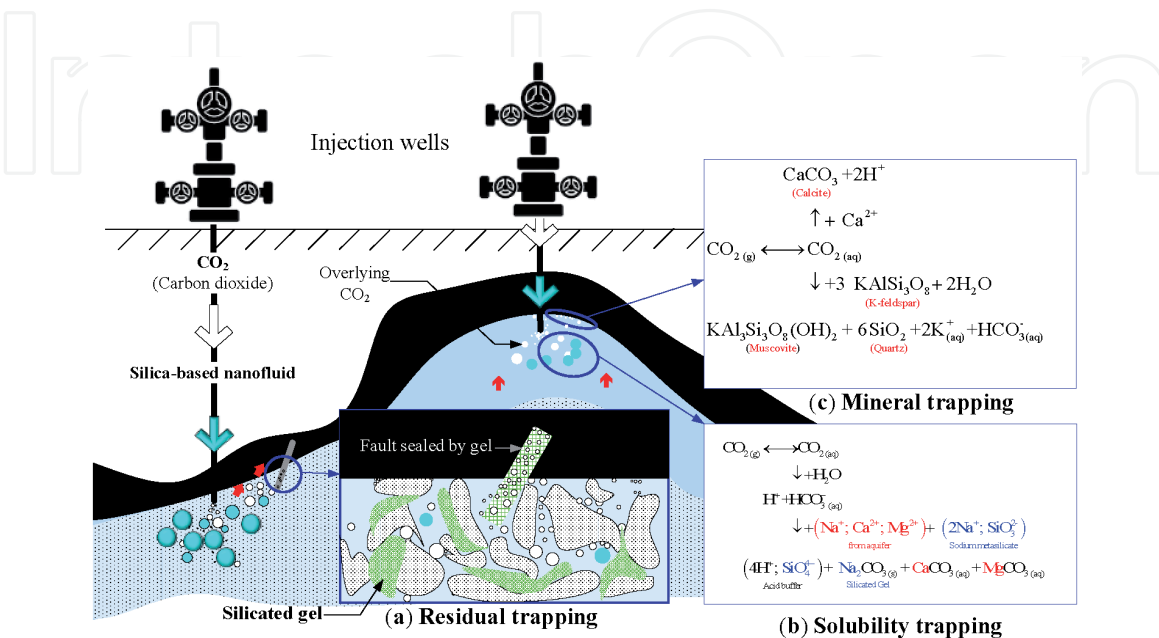

Figure 14.
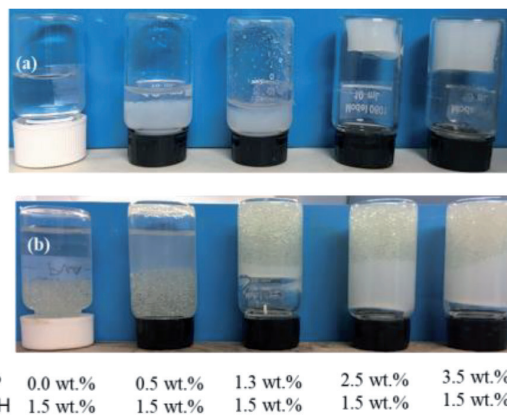*Conceptual enhancement of CO_2 sequestration by Si-NF injection.*

Figure 15.
Silicated-gel formed from Si-NP and polyvinyl alcohol without (a) porous medium and (b) in a porous medium.
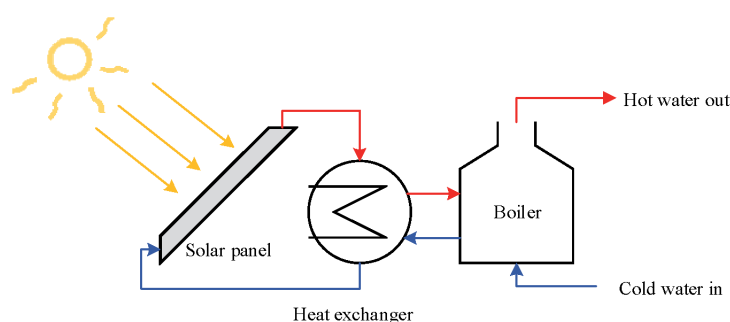

Figure 16.
Schematic representation of a thermal solar system for water heating applications.

Solar thermal energy consists in transforming photons into heat, which is collected and distributed by the means of devices called solar collectors [88]. A solar system usually has at least three components including the solar collector, a heat exchanger, and a thermal storage system (**Figure 16**).

Solar collectors use working fluids exposed to the solar irradiation. One of the most attractive candidates working fluid is water, given its price, its availability, and its eco-friendliness. The optimal temperature that can be obtained from a solar system depends on the type of solar collectors, which include flate-plate, parabolic through and parabolic dish collectors [89, 90].

4.3.2 Relevance of MO-NPs in solar thermal systems

The efficiency of a solar thermal systems is strongly related to the thermal efficiency of the working fluid, which is the ratio of useful energy effectively transferred. Ideal working fluids should exhibit peculiar thermophysical properties such as low viscosity, high thermal conductivity and high specific heat capacity, in addition to chemical stability [91]. The interest of MO-NPs for solar applications lies on their ability to enhance of the properties, which results in a significant improvement of the outlet temperature nand the net power produced within a solar thermal system.

The literature reports that MO nanofluids have a higher thermal conductivity than that water taken alone [92]. The replacement of water as Heat Transfer Fluid (HTF) by a SiO_2-water based nanofluid has demonstrated the ability to enhance the performance of a FP collector through the reduction of the viscosity, the enhancement of the specific heat capacity and the rise of the temperature of the HTF at the outlet temperature of the solar system [93].

A theoretical model assessing the performance of a solar thermal system using Al_2O_3-water based nanofluid as Direct Absorber Solar Collector (DASC) has shown an increase of 10% of the collector efficiency compared to water-based flat plate solar collectors operating in the same conditions [94]. However, the optical performance of MO-NF as DASC depends of the volume fraction of MO-NPs [95]. MO-NP can also be associated with photovoltaic devices within hybrid Photovoltaic Thermal (PV/T) systems.

In such configurations, the electrical and thermal energy are simultaneously generated by a photovoltaic module and the working fluid, respectively [96]. Furthermore, nanofluids, exhibiting magnetic properties, offer the possibility to increase the thermal conductivity of a working fluid upon the application of a magnetic field [97, 98]. Nano ferrofluids, standing amongst, were found to improve significantly the efficiency of the photothermal or PV/T systems [99].

However, the major challenge with such types of nanofluids is the formulation of stable working fluid. This is so because nano ferrofluids have the propensity either to agglomerate in solution [100] or to suffer from chemical instability [101]. The combination of Fe_3O_4 with other MO-NP in composite materials usually allows to overcome those limitations. Therefore, exploration of the thermophysical features of composite MO nanofluids is an interesting direction aiming at the optimization of solar thermal systems.

5. Concluding remarks

The present chapter has covered the topic of metal oxide nanoparticles (MO-NP) and nanocomposites (MO-NCP) and their application for carbon capture utilization and storage (CCUS). It was shown that MO-NP (or MO-NCP) can be synthesized using physical, chemical, and biological methods. Each approach is tuned to give a MO-NP (or MO-NCP) with specific features. Regardless the production route, it was highlighted the stability of the nanofluid was the main challenge.

In respect of CCUS application, the most prominent results were obtained from silica (SiO_2) and alumina (Al_2O_3) oxides. SiO_2-NP could alter the wettability in a manner to increase the production of heavy oil. Dispersed into polymeric base fluid, it was shown SiO_2-NP could yield a gel-structure, which can plug the large voids of formation, leading to either an increment of oil production or prevent the leakage of sequestered gases. On the other, Al_2O_3-NP and its silicate composite could delay the deposition in heavy materials during the oil production using carbon dioxide (CO_2) injection. On the other hand, it was shown that ferrous and ferric nanofluids could improve the heat transfer of the fluid, making them good candidate for solar thermal energy.

Acknowledgements

Conflict of interest

The authors declare no conflict of interest.

Funding

Author details

Ronald Nguele[1*], Katia Nchimi Nono[2] and Kyuro Sasaki[1]

1 Kyushu University, Fukuoka, Japan

2 University of Yaoundé I, Cameroon

*Address all correspondence to: nguele@mine.kyushu-u.ac.jp

IntechOpen

References

[1] Coey JMD, Venkatesan M, Xu H. Introduction to Magnetic Oxides. Functional Metal Oxides. 2013. p. 1-49.

[2] Yuan C, Wu H Bin, Xie Y, Lou XW (David). Mixed Transition-Metal Oxides: Design, Synthesis, and Energy-Related Applications. Angew Chemie Int Ed [Internet]. 2014 Feb 3;53(6):1488-504.

[3] Fang J, Xuan Y, Li Q. Preparation of three-dimensionally ordered macroporous perovskite materials. Chinese Sci Bull. 2011 Jul 1;56:2156-2161.

[4] Sadakane M, Ueda W. Three-Dimensionally Ordered Macroporous (3DOM) Perovskite Mixed Metal Oxides. In: Perovskites and Related Mixed Oxides. Weinheim, Germany: Wiley-VCH Verlag GmbH & Co. KGaA; 2015. p. 113-142.

[5] Merkel TJ, Herlihy KP, Nunes J, Orgel RM, Rolland JP, DeSimone JM. Scalable, shape-specific, top-down fabrication methods for the synthesis of engineered colloidal particles. Langmuir. 2010 Aug;26(16):13086-13096.

[6] Gerberich WW, Jungk JM, Mook WM. The Bottom-Up Approach To Materials By Design. In: Meyers MA, Ritchie RO, Sarikaya MBT-N and MD of AM, editors. Oxford: Elsevier Science Ltd; 2003. p. 211-220.

[7] Zhao X, Zheng B, Li C, Gu H. Acetate-derived ZnO ultrafine particles synthesized by spray pyrolysis. Powder Technol. 1998;100(1):20-23.

[8] Azurdia J, Marchal J, Laine R. Synthesis and Characterization of Mixed-Metal Oxide Nanopowders Along the CoO_x–Al_2O_3 Tie Line Using Liquid-Feed Flame Spray Pyrolysis. J Am Ceram Soc. 2006 Sep 1;89:2749-2756.

[9] Azurdia JA, McCrum A, Laine RM. Systematic synthesis of mixed-metal oxides in NiO–Co3O4, NiO–MoO_3, and NiO–CuO systems via liquid-feed flame spray pyrolysis. J Mater Chem. 2008;18(27):3249-3258.

[10] Chao LT, Wei M, MacManus-Driscoll JL. Synthesis and characterisation of nanocrystalline iron oxides via ultrasonic spray assisted chemical vapour deposition. J Phys Conf Ser. 2006 Feb 22;26(1):304-307.

[11] Suslick KS. Sonochemistry. Science (80). 1990 Mar 23;247(4949):1439-45.

[12] Kumar RV, Diamant Y, Gedanken A. Sonochemical Synthesis and Characterization of Nanometer-Size Transition Metal Oxides from Metal Acetates. Chem Mater. 2000 Aug 1;12(8):2301-2305.

[13] Díez-García MI, Manzi-Orezzoli V, Jankulovska M, Anandan S, Bonete P, Gómez R, et al. Effects of Ultrasound Irradiation on the Synthesis of Metal Oxide Nanostructures. Phys Procedia. 2015;63:85-90.

[14] Shi W, Song S, Zhang H. Hydrothermal synthetic strategies of inorganic semiconducting nanostructures. Chem Soc Rev. 2013;42(13):5714-5743.

[15] Ota J, Srivastava SK. Polypyrrole Coating of Tartaric Acid-Assisted Synthesized Bi_2S_3 Nanorods. J Phys Chem C. 2007 Aug 1;111(33):12260-12264.

[16] Yuan G, Cao Y, Zan N, Schulz HM, Gluyas J, Hao F, et al. Coupled mineral alteration and oil degradation in thermal oil-water-feldspar systems and implications for organic-inorganic interactions in hydrocarbon reservoirs. Geochim Cosmochim Acta. 2019;248:61-87.

[17] Thapa R, Maiti S, Rana TH, Maiti UN, Chattopadhyay KK. Anatase TiO$_2$ nanoparticles synthesis via simple hydrothermal route: Degradation of Orange II, Methyl Orange and Rhodamine B. J Mol Catal A Chem. 2012;363-364:223-229.

[18] Xiaoming F. Synthesis and Optical Absorption Properies of Anatase TiO$_2$ Nanoparticles via a Hydrothermal Hydrolysis Method. Rare Met Mater Eng. 2015 May;44(5):1067-1070.

[19] Tong H, Enomoto N, Inada M, Tanaka Y, Hojo J. Hydrothermal synthesis of mesoporous TiO$_2$-SiO$_2$ core-shell composites for dye-sensitized solar cells. Electrochim Acta. 2014 Jun 1;130:329-334.

[20] Lu J, Qi D, Deng C, Zhang X, Yang P. Hydrothermal synthesis of α-Fe$_2$O$_3$@SnO$_2$ core–shell nanotubes for highly selective enrichment of phosphopeptides for mass spectrometry analysis. Nanoscale . 2010;2(10):1892-1900.

[21] Parashar M, Shukla V, Singh R. Metal oxides nanoparticles via sol–gel method: a review on synthesis, characterization and applications. J Mater Sci Mater Electron. 2020 Mar;31.

[22] Li X-L, Peng Q, Yi J-X, Wang X, Li Y. Near monodisperse TiO$_2$ nanoparticles and nanorods. Chemistry. 2006;12(8):2383—2391.

[23] Zeng H, Rice PM, Wang SX, Sun S. Shape-Controlled Synthesis and Shape-Induced Texture of MnFe$_2$O$_4$ Nanoparticles. J Am Chem Soc. 2004 Sep 1;126(37):11458-11459.

[24] Chen JC, Chen W-C, Tien Y-C, Shih C-J. Effect of calcination temperature on the crystallite growth of cerium oxide nano-powders prepared by the co-precipitation process. J Alloy Compd. 2010 Apr;496:364-369.

[25] Fu C, Ravindra NM. Magnetic iron oxide nanoparticles: synthesis and applications. Bioinspired, Biomim Nanobiomaterials. 2012 Aug;1(4):229-244.

[26] Liu J, You D, Yu M, Li S. Preparation and characterization of hollow glass microspheres–cobalt ferrite core-shell particles based on homogeneous coprecipitation. Mater Lett. 2011;65(5):929-932.

[27] Ansari MA, Khan HM, Alzohairy MA, Jalal M, Ali SG, Pal R, et al. Green synthesis of Al$_2$O$_3$ nanoparticles and their bactericidal potential against clinical isolates of multi-drug resistant Pseudomonas aeruginosa. World J Microbiol Biotechnol. 2015 Jan 11;31(1):153-164.

[28] Senthilkumar S, Rajendran A. Biosynthesis of TiO$_2$ nanoparticles using Justicia gendarussa leaves for photocatalytic and toxicity studies. Res Chem Intermed. 2018;44(10):5923-5940.

[29] Fridman AA. Plasma chemistry. Cambridge; New York: Cambridge University Press; 2008.

[30] Petitpas G, Rollier J-D, Darmon A, Gonzalez-Aguilar J, Metkemeijer R, Fulcheri L. A comparative study of non-thermal plasma assisted reforming technologies. Int J Hydrogen Energy . 2007;32(14):2848-2867.

[31] Acayanka E, Tarkwa J-B, Nchimi KN, Voufouo SAY, Tiya-Djowe A, Kamgang GY, et al. Grafting of N-doped titania nanoparticles synthesized by the plasma-assisted method on textile surface for sunlight photocatalytic self-cleaning applications. Surfaces and Interfaces. 2019;

[32] Acayanka E, Kuete DS, Kamgang GY, Nzali S, Laminsi S, Ndifon PT. Synthesis, Characterization

and Photocatalytic Application of TiO2/SnO2 Nanocomposite Obtained Under Non-thermal Plasma Condition at Atmospheric Pressure. Plasma Chem Plasma Process. 2016 May 21;36(3):799-811.

[33] Acayanka E, Tarkwa J-B, Nchimi KN, Voufouo SAY, Tiya-Djowe A, Kamgang GY, et al. Grafting of N-doped titania nanoparticles synthesized by the plasma-assisted method on textile surface for sunlight photocatalytic self-cleaning applications. Surfaces and Interfaces. 2019 Dec;17:100361.

[34] Chemical Fundamentals of Hydrometallurgy. Hydrometallurgy. 2013. p. 21-64. (Wiley Online Books).

[35] Manivasakan P, Rajendran V, Rauta PR, Sahu BB, Panda BK. Direct Synthesis of Nano Alumina from Natural Bauxite. Adv Mater Res. 2009 Apr 1;67:143-148.

[36] Rayzman V, Aturin A, Pevzner I, Sizyakov V, Ni L, Filipovich I. Extracting Silica and Alumina from Low-Grade Bauxite. JOM. 2003 Jan 8;55:47-50.

[37] Akoh H, Tsukasaki Y, Yatsuya S, Tasaki A. Magnetic properties of ferromagnetic ultrafine particles prepared by vacuum evaporation on running oil substrate. J Cryst Growth. 1978 Dec 1;45:495-500.

[38] Phuoc TX, Soong Y, Chyu MK. Synthesis of Ag-deionized water nanofluids using multi-beam laser ablation in liquids. Opt Lasers Eng. 2007 Dec;45(12):1099-1106.

[39] Everett DH. Chapter 2. Why are Colloidal Dispersions Stable? I Basic Principles. In 1988. p. 16-29.

[40] Bolukbasi A, Ciloglu D. Pool boiling heat transfer characteristics of vertical cylinder quenched by SiO_2–water nanofluids. Int J Therm Sci. 2011 Jun 1;50(6):1013-1021.

[41] Darzi AAR, Farhadi M, Sedighi K, Shafaghat R, Zabihi K. Experimental investigation of turbulent heat transfer and flow characteristics of SiO_2/water nanofluid within helically corrugated tubes. Int Commun Heat Mass Transf. 2012 Nov 1;39(9):1425-1434.

[42] Kumar RS, Sharma T. Stability and rheological properties of nanofluids stabilized by SiO_2 nanoparticles and SiO_2-TiO_2 nanocomposites for oilfield applications. Colloids Surfaces A Physicochem Eng Asp. 2018 Feb;539:171-183.

[43] Nguele R, Sreu T, Inoue H, Sugai Y, Sasaki K. Enhancing Oil Production Using Silica-Based Nanofluids: Preparation, Stability, and Displacement Mechanisms. Ind Eng Chem Res. 2019 Aug;58(32):15045-15060.

[44] Suslick KS, Didenko Y, Fang MM, Hyeon T, Kolbeck KJ, McNamara III WB, et al. Acoustic cavitation and its consequences. Philos Trans R Soc A. 1999;357(1927):335-353.

[45] Xuan Y, Li Q. Heat transfer enhancement of nanofluids. Int J Heat Fluid Flow. 2000 Feb 1;21(1):58-64.

[46] Garg J, Poudel B, Chiesa M, Gordon JB, Ma JJ, Wang JB, et al. Enhanced thermal conductivity and viscosity of copper nanoparticles in ethylene glycol nanofluid. J Appl Phys. 2008 Apr 2;103(7):074301.

[47] Ngo I, Sasaki K, Nguele R, Sugai Y. Formation Damage Induced by Water-Based Alumina Nanofluids during Enhanced Oil Recovery: Influence of Postflush Salinity. ACS Omega. 2020 Oct 27;5(42):27103-27112.

[48] Ali N, Teixeira JA, Addali A. A Review on Nanofluids: Fabrication, Stability, and Thermophysical Properties. J Nanomater. 2018; 2018:1-33.

[49] Kato H, Nakamura A, Noda N. Determination of size distribution of silica nanoparticles: A comparison of scanning electron microscopy, dynamic light scattering, and flow field-flow fractionation with multiangle light scattering methods. Mater Express. 2014;4(2):144-152.

[50] Sidik NAC, Mohammed HA, Alawi OA, Samion S. A review on preparation methods and challenges of nanofluids. Int Commun Heat Mass Transf. 2014 May;54:115-125.

[51] Fazeli SA, Hosseini Hashemi SM, Zirakzadeh H, Ashjaee M. Experimental and numerical investigation of heat transfer in a miniature heat sink utilizing silica nanofluid. Superlattices Microstruct. 2012 Feb 1;51(2):247-264.

[52] Pang C, Jung J-Y, Lee JW, Kang YT. Thermal conductivity measurement of methanol-based nanofluids with Al_2O_3 and SiO_2 nanoparticles. Int J Heat Mass Transf. 2012 Oct 1;55(21-22):5597-5602.

[53] Devendiran DK, Amirtham VA. A review on preparation, characterization, properties and applications of nanofluids. Renew Sustain Energy Rev. 2016;60:21-40.

[54] Shah A, Fishwick R, Wood J, Leeke G, Rigby S, Greaves M. A review of novel techniques for heavy oil and bitumen extraction and upgrading. Energy Environ Sci. 2010;3(6):700.

[55] Or C, Sasaki K, Sugai Y, Nakano M, Imai M. Preliminary numerical modelling of CO_2 gas foaming in heavy oil and simulations of oil production from heavy oil reservoirs. Can J Chem Eng. 2016 Mar;94(3):576-585.

[56] Speight JG. Petroleum asphaltenes - Part 1: Asphaltenes, resins and the structure of petroleum. Oil Gas Sci Technol. 2004;59(5):467-477.

[57] Nguele R, Ghulami MR, Sasaki K, Said-Al Salim H, Widiatmojo A, Sugai Y, et al. Asphaltene Aggregation in Crude Oils during Supercritical Gas Injection. Energy and Fuels. 2016 Feb;30(2):1266-1278.

[58] Nguele R, Sasaki K, Ghulami MR, Sugai Y, Nakano M. Pseudo-phase equilibrium of light and heavy crude oils for enhanced oil recovery. J Pet Explor Prod Technol. 2016 Sep 20;6(3):419-432.

[59] Ngo I, Srisuriyachai F, Sasaki K, Sugai Y, Nguele R. Effects of Reversibility on Enhanced Oil Recovery Using Sodium Dodecylbenzene Sulfonate (SDBS). J Japan Pet Inst. 2019 Jul 1;62(4):188-198.

[60] Nguele R, Sasaki K, Salim HS, Sugai Y. Physicochemical and microemulsion properties of dimeric quaternary ammonium salts with trimethylene spacer for enhanced oil recovery. Colloid Polym Sci. 2015 Dec 2;293(12):3487-3497.

[61] Nguele R, Sasaki K, Sugai Y, Said Al-Salim H, Ueda R. Mobilization and displacement of heavy oil by cationic microemulsions in different sandstone formations. J Pet Sci Eng. 2017 Aug;157:1115-1129.

[62] Santanna VC, Curbelo FDS, Castro Dantas TN, Dantas Neto AA, Albuquerque HS, Garnica AIC. Microemulsion flooding for enhanced oil recovery. J Pet Sci Eng. 2009 Jun;66(3-4):117-120.

[63] Nguele R, Sasaki K, Salim HS-A, Sugai Y, Widiatmojo A, Nakano M. Microemulsion and phase behavior properties of (Dimeric ammonium surfactant salt – heavy crude oil – connate water) system. J Unconv Oil Gas Resour. 2016 Jun;14:62-71.

[64] Bera A, Mandal A. Microemulsions: a novel approach to enhanced oil

recovery: a review. J Pet Explor Prod Technol. 2015 Sep;5(3):255-268.

[65] Thomas S. Enhanced oil recovery-an overview. Oil Gas Sci Technol. 2008;63(1):9-19.

[66] Ansah EO, Sugai Y, Nguele R, Sasaki K. Integrated microbial enhanced oil recovery (MEOR) simulation: Main influencing parameters and uncertainty assessment. J Pet Sci Eng. 2018 Dec;171:784-793.

[67] Purwasena IA, Astuti DI, Syukron M, Amaniyah M, Sugai Y. Stability test of biosurfactant produced by Bacillus licheniformis DS1 using experimental design and its application for MEOR. J Pet Sci Eng. 2019 Dec 1;183.

[68] Ansah EO, Vo Thanh H, Sugai Y, Nguele R, Sasaki K. Microbe-induced fluid viscosity variation: field-scale simulation, sensitivity and geological uncertainty. J Pet Explor Prod Technol. 2020 Jun 1;10(5):1983-2003.

[69] Ogolo NA, Olafuyi OA, Onyekonwu MO. Enhanced Oil Recovery Using Nanoparticles. In: SPE Saudi Arabia Section Technical Symposium and Exhibition. Society of Petroleum Engineers; 2012.

[70] Hendraningrat L, Li S, Torsæter O. A coreflood investigation of nanofluid enhanced oil recovery. J Pet Sci Eng. 2013 Nov;111:128-138.

[71] Li S, Hendraningrat L, Torsaeter O. Improved Oil Recovery by Hydrophilic Silica Nanoparticles Suspension: 2-Phase Flow Experimental Studies. In: International Petroleum Technology Conference. International Petroleum Technology Conference; 2013.

[72] Giraldo J, Benjumea P, Lopera S, Cortés FB, Ruiz MA. Wettability Alteration of Sandstone Cores by Alumina-Based Nanofluids. Energy & Fuels. 2013 Jul;27(7):3659-3665.

[73] Kothari N, Raina B, Chandak KB, Iyer V, Mahajan HP. Application Of Ferrofluids For Enhanced Surfactant Flooding In IOR. In: SPE EUROPEC/ EAGE Annual Conference and Exhibition. Society of Petroleum Engineers; 2010.

[74] Tarek M, El-Banbi AH. Comprehensive Investigation of Effects of Nano-Fluid Mixtures to Enhance Oil Recovery. In: SPE North Africa Technical Conference and Exhibition. Society of Petroleum Engineers; 2015.

[75] Haroun MR, Alhassan S, Ansari AA, Al Kindy NAM, Abou Sayed N, Abdul Kareem BA, et al. Smart Nano-EOR Process for Abu Dhabi Carbonate Reservoirs. In: Abu Dhabi International Petroleum Conference and Exhibition. Society of Petroleum Engineers; 2012. p. 1-13.

[76] Donaldson EC, Tiab DECD, Donaldson EC. Petrophysics: Theory and Practice of Measuring Reservoir Rock and Fluid Transport Properties. 2nd ed. Book. Gulf Professional Pub./ Elsevier; 2004. 898 p.

[77] Tola S, Sasaki K, Sugai Y. Wettability alteration of sandstone with zinc oxide nano-particles. In: 23rd Formation Evaluation Symposium of Japan 2017. 2017.

[78] Romero Z, Disney R, Acuna HM, Cortes F, Patino JE, Cespedes Chavarro C, et al. Application and evaluation of a nanofluid containing nanoparticles for asphaltenes inhibition in well CPSXL4. In: OTC Brasil. Offshore Technology Conference; 2013.

[79] Ibrahim HH, Idem RO. Interrelationships between asphaltene precipitation inhibitor effectiveness, asphaltenes characteristics, and precipitation behavior during n-heptane (light paraffin hydrocarbon)-induced

asphaltene precipitation. Energy and Fuels. 2004 Jul;18(4):1038-1048.

[80] Goual L. Petroleum Asphaltenes. In: Manar El-Sayed Abdul-Raouf, editor. Crude Oil Emulsions- Composition Stability and Characterization. InTech; 2012. p. 27-42.

[81] Salmawati S, Sasaki K, Sugai Y, Yousefi-Sahzabi A. Estimating a baseline of soil CO_2 flux at CO_2 geological storage sites. Environ Monit Assess. 2019 Sep 14;191(9):563.

[82] Yousefi-Sahzabi A, Sasaki K, Yousefi H, Pirasteh S, Sugai Y. GIS aided prediction of CO_2 emission dispersion from geothermal electricity production. J Clean Prod. 2011 Nov 1;19(17-18):1982-1993.

[83] Sasaki K, Susanto V, Anggara F, Yousefi-Sahzabi A, Sugai Y, Kawamura T, Et Al. Few Considerations on Problems of CO_2 Geological Storage with Carbon Circulation and Proposal of An Integrated Regional Energy System considering Low Carbon Society. J MMIJ. 2015 Aug 1 [cited 2019 Sep 20];131(8_9):503-8.

[84] Ajayi T, Gomes JS, Bera A. A review of CO2 storage in geological formations emphasizing modeling, monitoring and capacity estimation approaches. Pet Sci [Internet]. 2019 Jul 8 [cited 2019 Sep 19];1-36. Available from: http://link.springer.com/10.1007/s12182-019-0340-8

[85] Ansah EO, Nguele R, Sugai Y, Sasaki K. Predicting the antagonistic effect between albite-anorthite synergy and anhydrite on chemical enhanced oil recovery: effect of inorganic ions and scaling. J Dispers Sci Technol. 2020 Dec 31;42(1):21-32.

[86] Serrano E, Rus G, García-Martínez J. Nanotechnology for sustainable energy. Vol. 13, Renewable and Sustainable Energy Reviews. Pergamon; 2009. p. 2373-2384.

[87] Kannan N, Vakeesan D. Solar energy for future world: - A review. Renew Sustain Energy Rev. 2016;62:1092-1105.

[88] Tian Y, Zhao CY. A review of solar collectors and thermal energy storage in solar thermal applications. Appl Energy. 2013;104:538-553.

[89] Reddy KS, Kamnapure NR, Srivastava S. Nanofluid and nanocomposite applications in solar energy conversion systems for performance enhancement: a review. Int J Low-Carbon Technol. 2017 Mar;12(1):1-23.

[90] Tchanche BF, Lambrinos G, Frangoudakis A, Papadakis G. Low-grade heat conversion into power using organic Rankine cycles – A review of various applications. Renew Sustain Energy Rev. 2011;15(8):3963-3979.

[91] Axaopoulos PJ. Solar Thermal Conversion: Active Solar Systems. Simmetria Publications; 2011.

[92] Lee S, Choi SU-S, Li S, Eastman JA. Measuring Thermal Conductivity of Fluids Containing Oxide Nanoparticles. J Heat Transfer. 1999 May 1;121(2):280-289.

[93] Akhatov JS, Mirzaev SZ, Halimov AS, Telyaev SS, Juraev ET. Study of the possibilities of thermal performance enhancement of flat plate solar water collectors by using of nanofluids as heat transfer fluid. Appl Sol Energy. 2017;53(3):250-257.

[94] Tyagi H, Phelan P, Prasher R. Predicted Efficiency of a Low-Temperature Nanofluid-Based Direct Absorption Solar Collector. J Sol Energy Eng Asme - J Sol Energy Eng. 2009 Nov;131.

[95] Karami M, Akhavan-Bahabadi MA, Delfani S, Raisee M. Experimental investigation of CuO nanofluid-based

Direct Absorption Solar Collector for residential applications. Renew Sustain Energy Rev. 2015;52:793-801.

[96] Michael JJ, Iniyan S. Performance analysis of a copper sheet laminated photovoltaic thermal collector using copper oxide – water nanofluid. Sol Energy. 2015;119:439-451.

[97] Shima PD, Philip J. Tuning of Thermal Conductivity and Rheology of Nanofluids Using an External Stimulus. J Phys Chem C. 2011 Oct 20;115(41):20097-20104.

[98] Lajvardi M, moghimi rad J, Hadi I, Gavili A, Isfahani T, Zabihi F, et al. Experimental investigation for enhanced ferrofluid heat transfer under magnetic field effect. J Magn Magn Mater. 2010 Nov;322:3508-13.

[99] Ghadiri M, Sardarabadi M, Pasandideh-fard M, Moghadam AJ. Experimental investigation of a PVT system performance using nano ferrofluids. Energy Convers Manag. 2015;103:468-476.

[100] Smith MJ, Ho VHB, Darton NJ, Slater NKH. Effect of Magnetite Nanoparticle Agglomerates on Ultrasound Induced Inertial Cavitation. Ultrasound Med Biol. 2009;35(6):1010-1014.

[101] Lagoeiro Le. Transformation of magnetite to hematite and its influence on the dissolution of iron oxide minerals. J Metamorph Geol. 1998 May;16(3):415-423.